

An Efficient Fast Beamforming Algorithm for Sidelobe Suppression and Gain Loss Limitation

Xiaoyu Yao¹, Quan Gao, Zhanwen Wang, Li Wei², *Member, IEEE*, Lan Lan³, *Senior Member, IEEE*, and Wei E. I. Sha⁴, *Fellow, IEEE*

Abstract—This work investigates a deterministic transmit beamforming algorithm for sidelobe suppression under a predefined mainlobe gain loss. By enforcing the unit-norm constraint via the Lagrange multiplier method, the problem is formulated as a quadratic eigenvalue problem that yields a numerical solution without iterative optimization. The algorithm also supports asymmetric sidelobe control and null steering, offering flexible beampattern shaping. Simulation results under various gain loss constraints demonstrate that the proposed method achieves up to 28.70% relative reduction in the sidelobe power compared with classical tapering window functions and 16.13% compared with gradient-based algorithms, while achieving comparable peak sidelobe levels.

Index Terms—Sidelobe suppression, mainlobe gain, beamforming algorithm, Lagrange multiplier method.

I. INTRODUCTION

WITH the rise of 6G applications, wireless communication systems face unprecedented demands for capacity, latency, and reliability. Millimeter-wave (mmWave) and massive multiple-input multiple-output (MIMO) technologies have become essential to address these demands, yet mmWave signals suffer from severe path loss and blockage compared with microwave signals [1]. Beamforming using large-scale antenna arrays mitigates these issues by generating highly directional beams, but the resulting narrow coverage requires dynamic adaptation. Although dynamic antenna architectures [2], [3], [4] offer a hardware-level solution, their high implementation complexity and limited reconfiguration speed motivate the development of fast and robust transmit beamforming algorithms with real-time response.

Sidelobe suppression is a key objective in beamforming design to reduce power leakage and interference, but it often trades off with the mainlobe gain. Classic tapering window functions [5] are simple and preserve acceptable mainlobe gain, albeit at the cost of adaptability and flexibility. More flexible optimization-based approaches, including gradient-based

Received 14 January 2026; accepted 9 February 2026. Date of publication 11 February 2026; date of current version 24 February 2026. The associate editor coordinating the review of this letter and approving it for publication was S. Schwarz. (*Corresponding author: Wei E. I. Sha.*)

Xiaoyu Yao is with the Polytechnic Institute, Zhejiang University, Hangzhou 310015, China (e-mail: xiaoyu-yao@zju.edu.cn).

Quan Gao and Zhanwen Wang are with the College of Information Science and Electronic Engineering, Zhejiang University, Hangzhou 310027, China (e-mail: quangao@zju.edu.cn; zw_wang@zju.edu.cn).

Li Wei is with the School of Electrical and Electronics Engineering, Nanyang Technological University, Singapore 639798 (e-mail: l_wei@ntu.edu.sg).

Lan Lan is with the National Key Laboratory of Radar Signal Processing, Xidian University, Xi'an 710071, China (e-mail: lanlan@xidian.edu.cn).

Wei E. I. Sha is with Zhejiang Key Laboratory of Intelligent Electromagnetic Control and Advanced Electronic Integration, Zhejiang University, Hangzhou 310027, China (e-mail: weisha@zju.edu.cn).

Digital Object Identifier 10.1109/LCOMM.2026.3663709

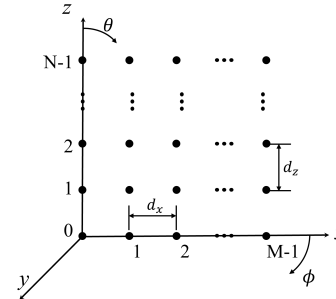


Fig. 1. Schematic diagram of the uniform plane array.

algorithms [6], [7] and metaheuristic algorithms [8], [9], have been investigated, but they may suffer from convergence issues. Matrix-based beampattern synthesis methods [10], [11] formulate sidelobe suppression as a quadratic or covariance shaping problem, which is commonly solved via convex optimization at the cost of iterative solvers and high computational complexity. Moreover, another widely adopted criterion is maximization of the signal-to-interference-plus-noise ratio (SINR). Adaptive methods [12] such as MVDR and LCMV optimize this objective and are primarily receiver-oriented, and are thus not directly applicable to deterministic transmit beampattern control.

Here, we propose a deterministic transmit beamforming algorithm for sidelobe power suppression with a controllable mainlobe gain loss. By a dedicated construction of the weight vector, the mainlobe subspace is decoupled from the sidelobe one, which allows the sidelobe power to be minimized while explicitly constraining the gain loss to a predefined value. This structural decoupling enables a deterministic solution for the optimal beamforming weights under a fixed gain loss, rather than relying on iterative optimization.

By enforcing the unit-norm constraint via the classical Lagrange multiplier method, we transform the optimization problem into a quadratic eigenvalue problem (QEP) which can be numerically solved without iterative optimization [13]. Moreover, additional flexibility can be obtained by incorporating simple iterative updates on the weighted integrated sidelobe level (ISL), enabling flexible beampattern shaping or enhanced peak sidelobe level (PSL) control. Simulation results have verified the effectiveness and stability of the proposed algorithm under various gain loss constraints and sidelobe suppression scenarios. It is noted that the proposed algorithm is developed in the classical single-beam scenario, which also serves as a fundamental building block for more general multi-beam beamforming designs.

Notation: We let a or A , \mathbf{a} , \mathbf{A} represent the scalar, vector, and matrix; $(\cdot)^T$, $(\cdot)^*$, $(\cdot)^H$, and $(\cdot)^{-1}$ denote the transpose

operator, conjugate operator, Hermitian transpose operator, and inverse of a matrix; $\max\{a, b\}$ denotes the maximum of a and b ; \mathbf{I} and \mathbf{O} denote the identity matrix and the all-zero matrix.

II. PROBLEM FORMULATION

Consider a uniform planar array (UPA) in xoz plane with M elements in the horizontal direction, N elements in the vertical direction, and $P = M \times N$. The spacings between the elements in the horizontal and vertical directions are d_x and d_z , respectively. The total beampattern of the UPA in any direction (θ, ϕ) can be expressed as:

$$\begin{aligned} E_{\text{total}}(\theta, \phi) &= \sum_{m=0}^{M-1} \sum_{n=0}^{N-1} w_{m,n} E_{\text{unit}}(\theta, \phi) e^{j\left(\frac{2\pi}{\lambda_0} m d_x \sin\theta \cos\phi + \frac{2\pi}{\lambda_0} n d_z \cos\theta\right)}, \end{aligned} \quad (1)$$

where λ_0 represents the free-space wavelength, $w_{m,n}$ represents the complex weight of the elements at position (m, n) , $E_{\text{unit}}(\theta, \phi)$ represents the isolated pattern of the array element for an ideal case or active element pattern for a practical case, θ is the elevation angle measured from the z -axis, and ϕ is the azimuth angle measured in the xoy plane (as shown in Fig. 1).

Extract the beamforming weight vector \mathbf{w} from (1) as $\mathbf{w} = [w_{0,0} \ w_{0,1} \ \dots \ w_{M-1,N-1}]^T$, then the power in the target direction (θ_0, ϕ_0) can be expressed as the quadratic form:

$$P_{\text{main}}(\mathbf{w}) = |E_{\text{total}}(\theta_0, \phi_0)|^2 = \mathbf{w}^H \mathbf{R}_{\text{main}} \mathbf{w}, \quad (2)$$

where $\mathbf{R}_{\text{main}} = \mathbf{e}(\theta_0, \phi_0) \mathbf{e}^H(\theta_0, \phi_0) \in \mathbb{C}^{P \times P}$ is the covariance matrix of the array response in the target direction, and the array response $\mathbf{e}(\theta_0, \phi_0)$ can be written as:

$$\mathbf{e}(\theta_0, \phi_0) = \begin{bmatrix} E_{\text{unit}}(\theta_0, \phi_0) \\ E_{\text{unit}}(\theta_0, \phi_0) e^{j\frac{2\pi}{\lambda_0} d_z \cos\theta_0} \\ \vdots \\ E_{\text{unit}}(\theta_0, \phi_0) e^{j\frac{2\pi}{\lambda_0} [(M-1)d_x \sin\theta_0 \cos\phi_0 + (N-1)d_z \cos\theta_0]} \end{bmatrix}^T \quad (3)$$

To find the weight vector that steers towards the target direction and maximizes the mainlobe gain, we consider the singular value decomposition (SVD):

$$\mathbf{R}_{\text{main}} = \mathbf{U} \Sigma \mathbf{U}^H. \quad (4)$$

Since $\text{rank}(\mathbf{R}_{\text{main}}) = 1$, it contains a single nonzero singular value σ_0 , whose corresponding singular vector \mathbf{w}_0 maximizes the mainlobe gain. All remaining singular vectors span the null space of \mathbf{R}_{main} , which is orthogonal to the target direction.

Physically, any weight component lying in this orthogonal subspace does not radiate toward the mainlobe. The mainlobe gain is determined by the projection onto \mathbf{w}_0 , while the remaining degrees of freedom are exploited for sidelobe suppression. In essence, this subspace decomposition enables a structural decoupling between the mainlobe control and sidelobe shaping.

Accordingly, since \mathbf{w}_0 alone does not account for the radiation power in the interference regions (or the sidelobe regions), we further formulate the power leakage minimization

problem by minimizing the weighted ISL, subject to the mainlobe gain and unit-norm constraints, as given by:

$$\begin{aligned} \min_{\{\mathbf{w}\}} P(\mathbf{w}) &= \mathbf{w}^H \mathbf{R}_{\text{side}} \mathbf{w} \\ \text{s.t. } \mathbf{w}^H \mathbf{R}_{\text{main}} \mathbf{w} &= 10^{-\frac{a}{10}} \mathbf{w}_0^H \mathbf{R}_{\text{main}} \mathbf{w}_0, \\ \mathbf{w}^H \mathbf{w} &= 1, \end{aligned} \quad (5)$$

where $\mathbf{R}_{\text{side}} = \sum_{i=1}^K \alpha_i \mathbf{e}(\theta_i, \phi_i) \mathbf{e}^H(\theta_i, \phi_i) \in \mathbb{C}^{P \times P}$, K is the number of sampling points depending on the selection of the interference region, and α_i is ISL weight constant controlling the suppression level at different angles. The variable a denotes the allowable mainlobe gain loss in decibels (dB). Using the standard power-to-dB relationship, a gain loss of a dB corresponds to a linear scaling factor of $10^{-\frac{a}{10}}$.

III. THE PROPOSED ALGORITHM

To simplify the optimization problem in (5), we propose a new method to construct the weight vector which can directly fix the gain loss to a predefined value. Define $s = 10^{-\frac{a}{20}}$ and $\mathbf{x} \in \mathbb{C}^{(P-1) \times 1}$, the weight vector is constructed as:

$$\mathbf{w}^H = [s \ \mathbf{x}^H] \mathbf{U}^H. \quad (6)$$

where $\mathbf{U} \in \mathbb{C}^{P \times P}$ is the left singular matrix of \mathbf{R}_{main} . The scalar s acts on the singular vector \mathbf{w}_0 , thereby determining the mainlobe gain in the target direction. Meanwhile, the auxiliary vector \mathbf{x}^H acts on the orthogonal subspace, enabling sidelobe suppression without affecting the mainlobe.

Then by combining (4) and (6), we can obtain:

$$P_{\text{main}} = s^2 \sigma_0 = 10^{-\frac{a}{10}} \sigma_0. \quad (7)$$

Obviously, (7) shows that the vector \mathbf{x} is independent of the mainlobe gain. Let $\mathbf{R} = \mathbf{U}^H \mathbf{R}_{\text{side}} \mathbf{U} \in \mathbb{C}^{P \times P}$, the optimization problem can be formulated as follows:

$$\begin{aligned} \min_{\{\mathbf{x}\}} P_{\text{side}}(\mathbf{x}) &= [s \ \mathbf{x}^H] \mathbf{R} \begin{bmatrix} s \\ \mathbf{x} \end{bmatrix} \\ \text{s.t. } \mathbf{x}^H \mathbf{x} &= 1 - s^2. \end{aligned} \quad (8)$$

Then we express \mathbf{R} as a block matrix:

$$\mathbf{R} = \begin{bmatrix} r_{11} & \mathbf{r}_{12} \\ \mathbf{r}_{12}^H & \mathbf{R}_{22} \end{bmatrix} \quad (9)$$

Apply the Lagrange multiplier method to enforce the unit-norm constraint and rewrite the optimization problem:

$$\begin{aligned} \min_{\{\mathbf{x}\}} P_{\text{side}}(\mathbf{x}, \lambda) &= \mathbf{x}^H \mathbf{R}_{22} \mathbf{x} + s \mathbf{r}_{12} \mathbf{x} + s \mathbf{x}^H \mathbf{r}_{12}^H + s^2 r_{11} \\ &\quad - \lambda [\mathbf{x}^H \mathbf{x} - (1 - s^2)]. \end{aligned} \quad (10)$$

The optimal weight that meets the constraint conditions is obtained in the solutions that satisfy the following two equations:

$$\begin{aligned} \frac{\partial P}{\partial \mathbf{x}} &= (\mathbf{R}_{22} - \lambda \mathbf{I}) \mathbf{x}^* + s \mathbf{r}_{12}^T = 0, \\ \frac{\partial P}{\partial \lambda} &= \mathbf{x}^H \mathbf{x} - 1 + s^2 = 0. \end{aligned} \quad (11)$$

The \mathbf{x} corresponding to the smallest real-valued λ in the solutions is the optimal weight that minimizes the objective function [14].

Algorithm 1 Analytical Optimization Procedure

- 1: **Input:** Gain loss limitation s , power covariance matrix \mathbf{R}_{main} and \mathbf{R}_{side} ;
- 2: **Output:** Optimal pair (λ, \mathbf{x}) , optimal weight vector \mathbf{w} .
- 3: $\mathbf{U} \leftarrow \text{SVD}(\mathbf{R}_{\text{main}})$;
- 4: $\mathbf{R} \leftarrow \mathbf{U}^H \mathbf{R}_{\text{side}} \mathbf{U}$;
- 5: Extract r_{11} , \mathbf{r}_{12} , and \mathbf{R}_{22} from \mathbf{R} according to (9);
- 6: Obtain (λ, \mathbf{x}) from the QEP in (12);
- 7: $\mathbf{w}^H \leftarrow [s \quad \mathbf{x}^H] \mathbf{U}^H$.

Algorithm 2 Iterative Optimization Procedure

- 1: **Input:** Gain loss limitation s , power covariance matrix \mathbf{R}_{main} , ISL weight constants $\alpha_1, \alpha_2, \dots, \alpha_K$, sidelobe threshold mask \mathbf{G}_{th} ;
- 2: **Output:** Optimal pair (λ, \mathbf{x}) , optimal weight vector \mathbf{w} .
- 3: Initialize $t \leftarrow 0$, step size $\eta = 0.5$;
- 4: **repeat**
- 5: $\mathbf{R}_{\text{side}}^{(t)} \leftarrow \sum_{i=1}^K \alpha_i^{(t)} \mathbf{e}(\theta_i, \phi_i)^H \mathbf{e}(\theta_i, \phi_i)$;
- 6: Compute $\mathbf{w}^{(t)}$ using Algorithm 1;
- 7: Update $\alpha_i^{(t+1)}$ according to the update rule in (13);
- 8: $t \leftarrow t + 1$
- 9: **until** convergence or $t \geq T_{\text{max}}$
- 10: Return final weight vector: $\mathbf{w} \leftarrow \mathbf{w}^{(t)}$.

To avoid the nonlinear solution of λ , which generally requires iterative root-finding and increases computational complexity, we define that $\mathbf{u} = s(\mathbf{R}_{22} - \lambda \mathbf{I})^{-2} \mathbf{r}_{12}^H \in \mathbb{C}^{(P-1) \times 1}$. Then (11) can be transformed into:

$$(\mathbf{R}_{22} - \lambda \mathbf{I})^2 \mathbf{u} = \frac{s^2}{1 - s^2} \mathbf{r}_{12}^H \mathbf{r}_{12} \mathbf{u}. \quad (12)$$

By solving this generalized QEP in (12) for the minimum real-valued eigenvalue λ_{min} and the corresponding \mathbf{x}_{best} , the optimal weight $\mathbf{w}_{\text{best}}^H = [s \quad \mathbf{x}_{\text{best}}^H] \mathbf{U}^H$ can be obtained to minimize the objective function. (The complete derivation can be found in the **Appendix**).

To enable flexible beam pattern shaping under practical requirements, the proposed algorithm can be further improved with a simple iterative mechanism summarized in Algorithm 2.

The ISL weight constants are updated in a pointwise manner:

$$\begin{aligned} \alpha_i^{(t+1)} &= \alpha_i^{(t)} + \eta \max\{0, G^{(t)}(\theta_i, \phi_i) - G_{\text{th}}(\theta_i, \phi_i)\}, \\ G^{(t)}(\theta_i, \phi_i) &= 10 \log_{10} \left(\mathbf{w}^H \mathbf{e}^{(t)}(\theta_i, \phi_i)^H \mathbf{e}^{(t)}(\theta_i, \phi_i) \mathbf{w} \right), \end{aligned} \quad (13)$$

where $G^{(t)}(\theta_i, \phi_i)$ denotes the beam pattern gain at the i -th sampling point, $G_{\text{th}}(\theta_i, \phi_i)$ is the sidelobe threshold (in dB), η is the step-size parameter and we set $\eta = 0.5$.

IV. SIMULATION RESULTS

This section analyzes the performance of the proposed beamforming algorithm with simulations. A 20×12 half-wavelength-spaced UPA ($d_x = d_z = \lambda_0/2$) is adopted. Several representative examples are presented to demonstrate the

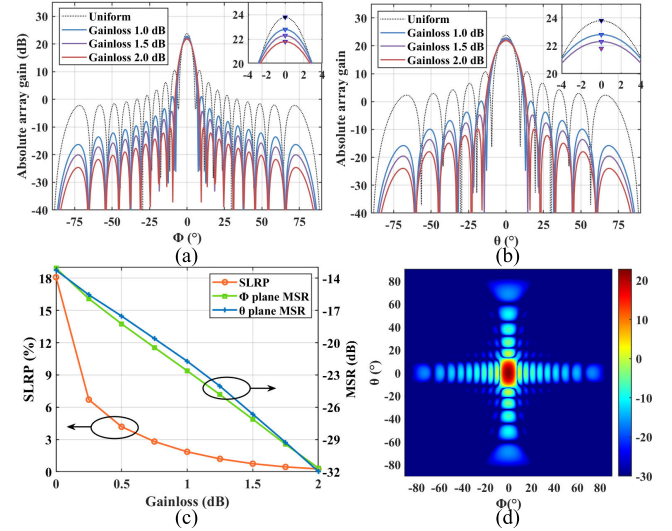


Fig. 2. Patterns of a $M \times N = 20 \times 12$ UPA with different mainlobe gain constraints. (a) Patterns cut in ϕ plane ($\theta = 90^\circ$). (b) Patterns cut in θ plane ($\phi = 90^\circ$). (c) The trade-off curves between the mainlobe gain loss and key sidelobe-related performance metrics. (d) Array gain distribution with a gain loss of 1.0 dB after optimization.

effects of different gain loss constraints and sidelobe suppression scenarios. The mainlobe region is set as $\phi \in [-9^\circ, 9^\circ]$ and $\theta \in [-15^\circ, 15^\circ]$. As for the sidelobe region, $K = 128064$ due to a uniform angular resolution of 0.5° . For fair comparison, the same angular sampling grid and sidelobe region definition are used for all compared methods.

A. Example 1: Beamforming With Different Gain Losses

By setting different values of s in the weight vector and all $\alpha_i = 1$, different mainlobe gain can be achieved. Fig. 2(a) and Fig. 2(b) show the resulting radiation patterns of the UPA in both ϕ and θ planes and the black dotted curve corresponds to the unconstrained maximum-gain pattern.

To evaluate the PSL performance, we adopt the Maximum Sidelobe Ratio (MSR), which is defined as the ratio between the highest sidelobe level and the mainlobe peak. And the Sidelobe Power Ratio (SLPR) is considered as an ISL-related metric, which indicates the proportion of the sidelobe power to total radiated power. Fig. 2(c) illustrates the trade-offs between the mainlobe gain loss and key sidelobe-related metrics. As the allowable gain loss increases from 0 to 2.0 dB, the SLPR decreases from 18.09% to 0.26%, corresponding to a relative reduction of over 98%. Meanwhile, the MSR in both the ϕ and θ planes improves approximately linearly, where each additional 0.25 dB gain loss yields about 2-2.5 dB sidelobe suppression.

As expected, there also exists an inherent trade-off between beamwidths, gain and sidelobe suppression shown in Fig. 2(a) and Fig. 2(b). Under a prescribed mainlobe gain loss constraint, the radiated energy within the mainlobe region is redistributed to achieve better sidelobe suppression resulting in a broader beamwidth when the gain loss constraint is relaxed. However, simulation results show that the 3-dB beamwidth increases by only about $1-2^\circ$, which is relatively small and remains acceptable for many practical applications such

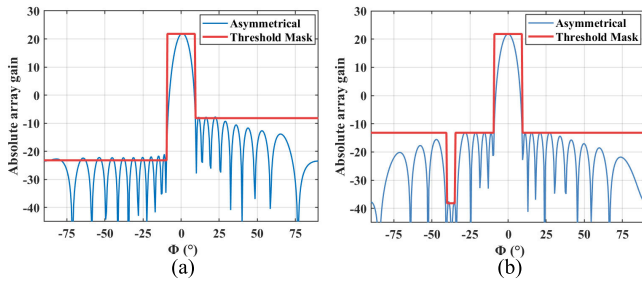


Fig. 3. Patterns of a $M \times N = 20 \times 12$ UPA with asymmetric sidelobe suppression. (a) Patterns cut in ϕ plane ($\theta = 90^\circ$) under left-side suppression. (b) Patterns cut in θ plane under a null constraint at $\phi = [-40^\circ, -35^\circ]$.

TABLE I

PERFORMANCE COMPARISON BETWEEN TAPERING WINDOW-BASED ALGORITHM AND THE IMPROVED ALGORITHM 2

Gain loss (dB)	Algorithm	SLPR(%)	ϕ plane MSR(dB)	θ plane MSR(dB)
1.3086	Chebyshev	2.23	-30.00	-30.00
1.3086	Proposed	1.59	-29.63	-29.61
1.3771	Taylor	1.61	-29.71	-30.24
1.3771	Proposed	1.25	-29.82	-29.82

as massive MIMO communications and interference-limited systems.

B. Example 2: Beamforming With Sidelobe Shaping

To demonstrate the flexibility of the proposed algorithm, the improved Algorithm 2 is adopted to synthesize beam patterns under a predefined gain loss of 2.0 dB. Two cases of asymmetric sidelobe suppression are achieved by appropriately updating the weighted ISL.

In the first case, the sidelobe level is constrained to -45 dB on the left side of the mainlobe and -30 dB on the right side. In the second case, a global sidelobe level of -35 dB is imposed, together with a deep null of -60 dB within the angular range $\phi \in [-40^\circ, -35^\circ]$.

For both cases, the designed threshold masks and the resulting beam patterns are shown in Fig. 3(a) and Fig. 3(b), verifying the effectiveness of the proposed algorithm in flexible sidelobe suppression and null steering for interference-limited or spatially selective communication scenarios.

C. Algorithm Performance Comparison

Firstly, classical tapering window functions are adopted as baselines, including the Chebyshev and Taylor windows, both configured to achieve a sidelobe suppression level of -30 dB.

For a fair comparison, the improved Algorithm 2 is employed to explicitly constrain the PSL, enabling evaluation under the same sidelobe suppression objective as the tapering window-based methods. Through the proposed algorithm, the same gain loss induced by each window function is easily imposed when computing the optimal weights.

Table I shows that the proposed Algorithm 2 achieves lower total sidelobe power than the tapering window-based methods under the same gain loss and comparable sidelobe levels. Compared with the Chebyshev window, the proposed algorithm provides an additional SLPR reduction of about 28.70%, while achieving similar MSR in both ϕ and θ planes.

TABLE II

PERFORMANCE COMPARISON BETWEEN THE GRADIENT-BASED ALGORITHM AND THE PROPOSED ALGORITHM 1

Gain loss (dB)	Algorithm	SLPR(%)	ϕ plane MSR(dB)	θ plane MSR(dB)
1.0	Iteration	1.86	-21.54	-22.56
1.0	Proposed	1.85	-21.72	-22.59
1.5	Iteration	0.75	-26.31	-26.70
1.5	Proposed	0.75	-26.64	-27.09
2.0	Iteration	0.31	-30.97	-31.22
2.0	Proposed	0.26	-31.97	-31.65

Relative to the Taylor window, an additional SLPR reduction of approximately 22.36% is also achieved with only marginal differences in MSR. These results indicate that the proposed algorithm is more effective in reducing the ISL while preserving comparable PSL performance.

As a second baseline, a gradient-based beamforming algorithm was implemented on an *Intel Xeon Gold 6240R CPU*. The gradient projection (GP) method [7] was adopted to enforce the unit-norm constraint. To improve convergence speed and robustness, the optimization was carried out using Adam optimizer and the objective function is as follows:

$$\begin{aligned} \min_{\{w\}} f(w) &= \frac{\beta}{K} w^H R_{\text{side}} w + (1 - \beta) \max\{g(w), 0\} \\ \text{s.t. } g(w) &= w^H R_{\text{main}} w - 10^{-\frac{\alpha}{10}} w_0^H R_{\text{main}} w_0, \\ &w^H w = 1, \end{aligned} \quad (14)$$

where β is used to balance the sidelobe power and the limited gain loss, and is set to $\beta = 0.9$ in all experiments.

To ensure a fair comparison, the gradient-based algorithm is randomly initialized and executed over 50 independent trials, with the best results reported. The learning rate is initialized to 0.5 and gradually decayed during the optimization. The algorithm terminates when either the maximum number of iterations is reached or the relative change of the objective function falls below the threshold.

Table II compares the proposed Algorithm 1 with the gradient-based algorithm under different gain loss constraints. When the gain loss is 2.0 dB, the proposed algorithm achieves a 16.13% relative reduction in the SLPR and improves the MSR by about 1 dB in ϕ plane. Under tighter constraints, both algorithms exhibit comparable SLPR performance, while the proposed algorithm still provides slightly improved MSR. These results demonstrate the effectiveness and robustness of the proposed algorithm in reducing total sidelobe power without relying on iterative optimization.

D. Computational Complexity and Numerical Stability Analysis

From a conservative perspective, the worst-case complexity of the proposed algorithm is $O(P^3)$ when dense eigenvalue decomposition (EVD) is employed. The SVD of the rank-one matrix R_{main} can reduce to extracting the dominant singular vector with $O(P^2)$ complexity. Furthermore, since only the smallest eigenvalue λ_{\min} is required, partial eigensolvers (e.g., Krylov subspace methods) can be applied, resulting in a reduced practical complexity.

In comparison, gradient-based algorithms typically exhibit a complexity of $O(P^2T)$, where T denotes the number of iterations, and require careful parameter tuning and are sensitive to initialization. Matrix-based beam pattern synthesis methods often rely on convex optimization solvers with high computational complexity, e.g., $O(P^4L^{2.5})$ in [10], where L is the number of constraints.

Regarding numerical stability, the linearized QEP is numerically ill-conditioned due to the coexistence of strong mainlobe and sidelobe components. However, the solution for the required eigenvalue λ_{\min} remains numerically stable due to its good separation from the rest of the spectrum as discussed in the **Appendix**.

V. CONCLUSION

This work proposes a deterministic single-beam transmit beamforming algorithm for sidelobe suppression while maintaining the mainlobe gain. By constructing the weight vector to decouple the mainlobe and sidelobe subspaces, the sidelobe power leakage minimization problem has been explicitly solved via a structured QEP without relying on iterative optimization. Simulation results have demonstrated that the proposed algorithm achieves lower sidelobe power and competitive PSL under the same gain loss constraints, compared with tapering window-based and gradient-based algorithms. Furthermore, by incorporating the weighted ISL and simple iterative updates, the proposed algorithm enables flexible beam pattern shaping, including asymmetric sidelobe suppression and null steering. Future work will investigate extensions to multi-beam or multi-user systems, as well as numerical conditioning and scalability issues for extremely large-scale arrays.

APPENDIX

In the optimization problem, we need to solve the following two equations:

$$\frac{\partial P}{\partial \mathbf{x}} = (\mathbf{R}_{22} - \lambda \mathbf{I}) \mathbf{x}^* + s \mathbf{r}_{12}^T = 0, \quad (\text{A1})$$

$$\frac{\partial P}{\partial \lambda} = \mathbf{x}^H \mathbf{x} - 1 + s^2 = 0. \quad (\text{A2})$$

It can be obtained from (A1):

$$\mathbf{x} = -s (\mathbf{R}_{22} - \lambda \mathbf{I})^{-1} \mathbf{r}_{12}^H. \quad (\text{A3})$$

Applying the substitution method, (A2) would be transformed into a nonlinear solution problem in terms of λ :

$$s^2 \mathbf{r}_{12}^H (\mathbf{R}_{22} - \lambda \mathbf{I})^{-2} \mathbf{r}_{12}^H = 1 - s^2. \quad (\text{A4})$$

Define that

$$\mathbf{u} = s (\mathbf{R}_{22} - \lambda \mathbf{I})^{-2} \mathbf{r}_{12}^H. \quad (\text{A5})$$

Then (A4) can be transformed into:

$$\frac{s}{1 - s^2} \mathbf{r}_{12}^H \mathbf{u} = 1. \quad (\text{A6})$$

Combined with the definition of \mathbf{u} and (A6), it can also be obtained that:

$$(\mathbf{R}_{22} - \lambda \mathbf{I})^2 \mathbf{u} = s \mathbf{r}_{12}^H = \frac{s^2}{1 - s^2} \mathbf{r}_{12}^H \mathbf{r}_{12}^H \mathbf{u}. \quad (\text{A7})$$

Define $\mathbf{M} = \mathbf{I}$, $\mathbf{C} = -2\mathbf{R}_{22}$ and $\mathbf{N} = \mathbf{R}_{22}^2 - \frac{s^2}{1-s^2} \mathbf{r}_{12}^H \mathbf{r}_{12}$, then (A7) can be transformed into a quadratic characteristic equation:

$$(\lambda^2 \mathbf{M} + \lambda \mathbf{C} + \mathbf{N}) \mathbf{u} = 0. \quad (\text{A8})$$

Note that \mathbf{N} is Hermitian but generally indefinite, as it consists of a positive semidefinite term and a scaled rank-one subtraction. Due to the coexistence of strong mainlobe and sidelobe components, the resulting eigenvalue problem may exhibit ill-conditioning.

Nevertheless, the particular structure of \mathbf{N} leads to a well-separated minimum eigenvalue λ_{\min} , which can be computed in a numerically stable manner, despite the overall ill-conditioning. The resulting QEP can be solved via standard linearization method:

$$\begin{bmatrix} -\mathbf{C} & -\mathbf{N} \\ \mathbf{I} & \mathbf{O} \end{bmatrix} \begin{bmatrix} \lambda \mathbf{u} \\ \mathbf{u} \end{bmatrix} = \lambda \begin{bmatrix} \mathbf{M} & \mathbf{O} \\ \mathbf{O} & \mathbf{I} \end{bmatrix} \begin{bmatrix} \lambda \mathbf{u} \\ \mathbf{u} \end{bmatrix}. \quad (\text{A9})$$

Solving this generalized QEP and obtaining the minimum real-valued eigenvalue λ_{\min} and the corresponding \mathbf{x}_{best} , the optimal weight $\mathbf{w}_{\text{best}}^H = [s \quad \mathbf{x}_{\text{best}}^H] \mathbf{U}^H$ is the solution that minimizes the objective function.

REFERENCES

- [1] A. H. Naqvi and S. Lim, "Review of recent phased arrays for millimeter-wave wireless communication," *Sensors*, vol. 18, no. 10, p. 3194, Sep. 2018.
- [2] G. Oliveri, P. Rocca, M. Salucci, D. Erricolo, and A. Massa, "Multi-scale single-bit RP-EMS synthesis for advanced propagation manipulation through system-by-design," *IEEE Trans. Antennas Propag.*, vol. 70, no. 10, pp. 8809–8824, Oct. 2022.
- [3] Z. Xiao et al., "Channel estimation for movable antenna communication systems: A framework based on compressed sensing," *IEEE Trans. Wireless Commun.*, vol. 23, no. 9, pp. 11814–11830, Sep. 2024.
- [4] L. Zhu, W. Ma, Z. Xiao, and R. Zhang, "Performance analysis and optimization for movable antenna aided wideband communications," *IEEE Trans. Wireless Commun.*, vol. 23, no. 12, pp. 18653–18668, Dec. 2024.
- [5] M. Zatzman, "Low sidelobe taper choice for wideband adaptive arrays," in *Proc. Antennas Propag. Soc. Int. Symp.*, 1998, pp. 192–194.
- [6] X. Jiang, W.-J. Zeng, A. Yasooharan, H. C. So, and T. Kirubarajan, "Quadratically constrained minimum dispersion beamforming via gradient projection," *IEEE Trans. Signal Process.*, vol. 63, no. 1, pp. 192–205, Jan. 2015.
- [7] J.-C. Chen, "Gradient projection-based alternating minimization algorithm for designing hybrid beamforming in millimeter-wave MIMO systems," *IEEE Commun. Lett.*, vol. 23, no. 1, pp. 112–115, Jan. 2019.
- [8] H. Li et al., "Beam space generalized sidelobe canceller algorithm based on particle swarm optimization," *Syst. Eng. Electron.*, vol. 44, no. 10, pp. 3037–3045, 2022.
- [9] J. Zhang, J. Chu, Y. Liu, and W. Zhang, "Suppression of peak sidelobe level in linear symmetric antenna arrays using hybrid grey wolf and improved bat algorithm," *Prog. Electromagn. Res. Lett.*, vol. 119, pp. 85–90, 2024.
- [10] J. Li, Y. Xie, P. Stoica, X. Zheng, and J. Ward, "Beam pattern synthesis via a matrix approach for signal power estimation," *IEEE Trans. Signal Process.*, vol. 55, no. 12, pp. 5643–5657, Dec. 2007.
- [11] T. V. Luyen, N. V. Cuong, and P. D. Hung, "Convex optimization-based linear and planar array pattern nulling," *Prog. Electromagn. Res. M*, vol. 128, pp. 21–30, 2024.
- [12] J. Li and P. Stoica, *Robust Adaptive Beamforming*. Hoboken, NJ, USA: Wiley, 2006.
- [13] W. Gander, G. H. Golub, and U. von Matt, "A constrained eigenvalue problem," *Linear Algebra Appl.*, vols. 114–115, pp. 815–839, Mar. 1989.
- [14] W. Gander, "Least squares with a quadratic constraint," *Numerische Math.*, vol. 36, no. 3, pp. 291–307, Sep. 1980.